Computer simulation study of size-exclusion chromatography with simultaneous viscometry and light scattering measurements

C. Jackson* and W.W. Yau[☆]

E.I. du Pont de Nemours and Company, Central Research and Development, Experimental Station, P.O. Box 80228, Wilmington, DE 19880-0228 (USA)

ABSTRACT

The integration of an on-line viscosity or light scattering (LS) detector with size-exclusion chromatography (SEC) improves the accuracy with which polymer molecular mass distributions can be measured. The coupling of a viscometer and a light scattering detector in one SEC instrument potentially offers improved precision and dynamic range for SEC polymer conformation studies. However, the increased complexity of these experiments and the subsequent data handling introduce a number of problems not present in conventional SEC. A computer simulation of the multiple detector SEC experiment was developed in order to study these effects in detail. The computer model is described and preliminary data are presented to illustrate some of the additional features of SEC with multiple detectors.

INTRODUCTION

The addition of one or more molecular mass sensitive detectors to a size-exclusion chromatographic (SEC) system increases greatly the amount of information that can be determined in the analysis. Measurement of the light-scattering intensity and the sample concentration enables the molecular mass distribution to be determined directly [1,2] and measurement of the specific viscosity and sample concentration enables the intrinsic viscosity distribution (IVD) to be determined [3]. In both cases the measurement does not require column calibration. This information can be combined with the hydrodynamic volume derived from column calibration to provide measurements of a number of polymer properties. By using both molecular size and molecular mass, the accuracy of the distributions can be improved. In addition, polymer conformation and architecture can be studied across the molecular mass distribution. Several methods have been developed for combining molecular mass and molecular size information [4–7].

However, this wealth of information is obtained at the expense of the simplicity of conventional SEC, and complex computer-based algorithms often hide important features of the instrument signals. Each of the measured signals depends on different polymer solution properties, with different molecular mass sensitivity, and as a result has different measurement ranges. The combination of these signals in the

---

* Corresponding author.
☆ Present address: Henkel Corporation, Research and Development, 300 Brookside Avenue, Ambler, PA 19002, USA.

final results can introduce errors in the final measurement [5,8–17].

In order to gain a clearer understanding of how the nature of the raw data affects the results we developed a computer simulation of the SEC experiment. The model is described and some of the preliminary results are discussed.

METHODOLOGY

SEC–light scattering computer model

We start by describing the mass fraction w_x, of x-mer, in a given polymer sample by the Wesslau distribution [18],

$$w_x = \frac{1}{\beta\pi^{1/2}} \cdot \frac{1}{x} \exp\left(-\frac{1}{\beta^2}\ln^2\frac{x}{x_0}\right) \quad (1)$$

where $\beta^2 = \ln(x_w/x_n)^2$, x_w is the mass-average degree of polymerization, x_n is the number average, and the central value of the distribution, $x_0 = x_n \exp(\beta^2/4)$.

In SEC the mass fraction is measured as a function of the logarithm of molecular mass in which case the mass fraction w'_x is described by

$$w'_x = w_x \frac{dx}{d\ln x} = xw_x \quad (2)$$

so,

$$w'_x = \frac{1}{\beta\pi^{1/2}} \exp\left(-\frac{1}{\beta^2}\ln^2\frac{x}{x_0}\right) \quad (3)$$

It can be seen that w'_x is a symmetrical Gaussian with a variance given by

$$\sigma_x^2 = \frac{\beta^2}{2} \quad (4)$$

which is related to the sample molecular mass polydispersity as

$$\frac{x_w}{x_n} = e^{\sigma_x^2} \quad (5)$$

Fig. 1 shows the mass-fraction distribution plotted as a function of the logarithm of x.

In SEC the molecular mass is related to the column elution volume by a calibration curve of the form [19],

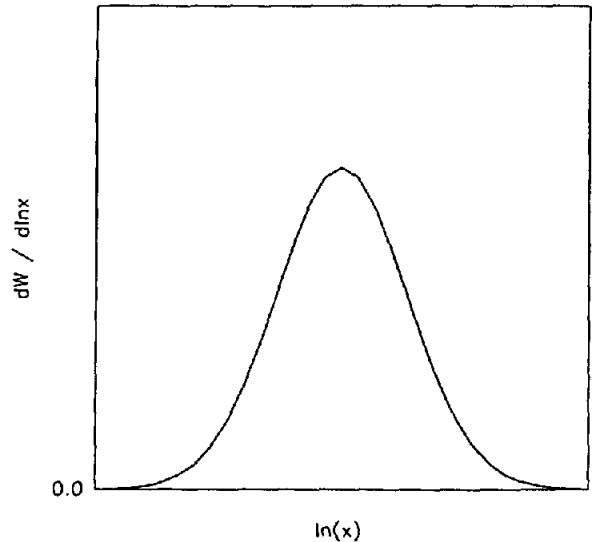$$M_t(V) = xM_0 = D_1 e^{-D_2 V} \quad (6)$$

Fig. 1. Wesslau distribution for the mass-fraction molecular mass distribution plotted as a function of the logarithm of the degree of polymerization, x.

where M_0 is the repeat unit molecular mass and D_1 and D_2 describe the calibration curve for a given column set. D_2 is the slope in a plot of log molecular mass against elution volume. Eqn. 3 can then be rewritten in terms of elution volume using eqn. 6, as,

$$w'_x(V) = \frac{1}{\sigma_V\sqrt{2\pi}} \exp\left[\frac{-(V-V_R)^2}{2\sigma_V^2}\right] \quad (7)$$

where the elution peak variance is related to the molecular mass variance by $\sigma_V = \sigma_x/D_2$, and V_R corresponds to the peak maximum in the concentration sensitive detector. Eqn. 7 describes the concentration detector elution profile for a sample with molecular mass distribution described by eqn. 1. Note that molecular mass decreases with increasing elution volume.

In the SEC–LS scattering experiment the sample can be considered to be at infinite dilution, in which case the intensity of scattered light at zero degrees from the incident beam is described by

$$I_{(\theta=0)}(V) = K^* M_t(V) w'_x(V) \quad (8)$$

where K^* is an optical constant for the scattering system [20]. The molecular mass at each volume

is described by eqn. 6, and the mass fraction distribution by eqn. 7, thus

$$I_{(\theta=0)}(V)$$

$$= K^* D_1 e^{-D_2 V} \frac{1}{\sigma_V \sqrt{2\pi}} \exp\left[\frac{-(V - V_R)^2}{2\sigma_V^2}\right] \quad (9)$$

It can be shown that this is also Gaussian with the same variance as the concentration detector response, but with a peak maximum, V_L, shifted to lower elution volume by an amount depending on the sample polydispersity and the slope of the calibration curve,

$$V_L = V_R - \sigma_V^2 D_2$$

$$= V_R - \frac{\sigma_x^2}{D_2} \quad (10)$$

SEC–viscometry computer model

In SEC–viscometry the specific viscosity of the eluting sample is measured. At infinite dilution this is related to the intrinsic viscosity by

$$\eta_{sp}(V) = [\eta](V) w_x'(V) \quad (11)$$

The intrinsic viscosity at each elution volume is given by eqn. 11 and the Mark–Houwink coefficients, K and a, which describe the empirical relationship between intrinsic viscosity and molecular mass [21],

$$[\eta](V) = K[M_t(V)]^a \quad (12)$$

Eqn. 11 can then be rewritten

$$\eta_{sp}(V) = K D_1^a e^{a(-D_2 V)} w_x'(V) \quad (13)$$

This also describes a symmetrical Gaussian with the same variance as the concentration detector response, but this time the peak maximum, V_V, is shifted to a lower elution volume determined by the value of the Mark–Houwink exponent as well as the polydispersity and the calibration curve slope,

$$V_V = V_R - a\sigma_x^2/D_2 \quad (14)$$

Fig. 2 shows the three signal traces, excess light-scattering intensity, specific viscosity, and differential refractive index, for a sample with a polydispersity of 2 and a Mark–Houwink exponent of 0.725. For a monodisperse standard
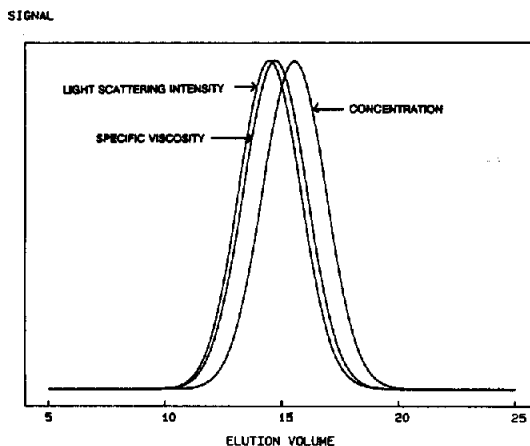

Fig. 2. Signal traces from the three detectors showing excess light-scattering intensity, specific viscosity, and differential refractive index, for a sample with a polydispersity of 2 and a Mark–Houwink exponent of 0.725. Elution volume in ml.

there is no volume shift between the three signal peaks and they all overlay. Fig. 3 illustrates an approximation to this situation with a nearly monodisperse sample of polydispersity 1.05

The universal calibration curve describes the hydrodynamic volume, HV, of the molecules at each elution volume [22],

$$HV_t(V) = [\eta]_t(V) \cdot M_t(V) = U_1 e^{-U_2 V} \quad (15)$$

where, from eqns. 6 and 13

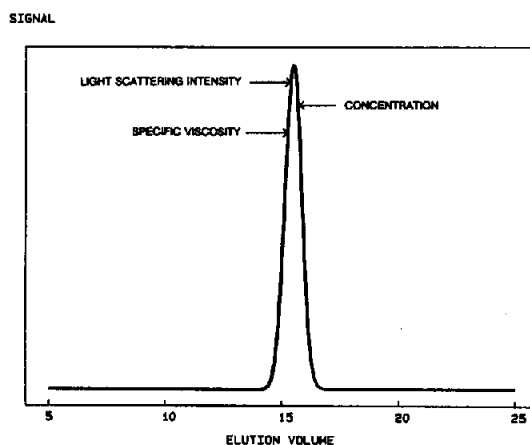$$U_1 = K D_1^{(a+1)} \quad (16)$$

Fig. 3. Signal traces from the three detectors for a nearly monodisperse sample, polydispersity 1.05. Elution volume in ml.

$$U_2 = (1 + a)D_2 \tag{17}$$

The intrinsic viscosity distribution can be used to characterize a polymer sample in a way analogous to the molecular mass distribution, with various statistical averages defined by [3]:

$$[\eta]_0 = \sum_i \frac{c_i}{c_i/[\eta]_i} \tag{18}$$

$$[\eta]_{+1} = \sum_i \frac{c_i[\eta]_i}{c_i} \tag{19}$$

$$[\eta]_{+2} = \sum_i \frac{c_i[\eta]_i^2}{c_i[\eta]_i} \tag{20}$$

Band broadening computer model

Band broadening in the system is modelled by the convolution of a Gaussian band spreading function

$$G(V) = \frac{1}{\sigma_B\sqrt{2\pi}} e^{-V^2/2\sigma_B^2} \tag{21}$$

where σ_B^2 is the peak variance due to band broadening, with the elution profile derived in eqn. 7. The experimentally determined concentration elution profile is then described by

$$w_x'(V) = \frac{1}{\sigma_T\sqrt{2\pi}} e^{\frac{-(V-V_0)^2}{2\sigma_T^2}} \tag{22}$$

where the total peak variance is given by $\sigma_T^2 = \sigma_V^2 + \sigma_B^2$.

The true mass-average and number-average molecular mass of an infinitesimal fraction at retention volume V are now given by [23]:

$$\overline{M_w}(V) = \frac{f(V - D_2\sigma_B^2)}{f(V)} e^{1/2(D_2\sigma_B)^2} M_t(V) \tag{23}$$

$$\overline{M_n}(V) = \frac{F(V)}{F(V + D_2\sigma_B^2)} e^{-1/2(D_2\sigma_B)^2} M_t(V) \tag{24}$$

where $F(V)$ is the experimental chromatogram broadened by the column dispersion process described by eqn. 21, where $F(V) = w_x'(V)$.

The effect of this broadening of the elution peak is a rotation of the calibration curve around the first moment of the concentration distribution. This leads to an effective mass-average molecular mass calibration curve defined by

$$x = D_1' e^{D_2'V} \tag{25}$$

where

$$D_1' = D_1 \exp\left[\frac{D_2\sigma_B^2(D_2\sigma_V^2 - 2V_0)}{2\sigma_T^2}\right] \tag{26}$$

$$D_2' = D_2\left(1 - \frac{\sigma_B^2}{\sigma_T^2}\right) \tag{27}$$

These expressions can also be used to define an effective mass-average intrinsic viscosity calibration curve,

$$[\eta](V) = E_1' e^{E_2'V} \tag{28}$$

where

$$E_1' = KD_1'^a \tag{29}$$

$$E_2' = aD_2' \tag{30}$$

The model described can be used to generate light-scattering intensity, specific viscosity, and differential refractive index data for samples with different Mark–Houwink relationships and with different amounts of band broadening. Mixtures of up to three peaks with differing polydispersities can be generated. The raw signal tracings can then be used to calculate results using different detector combinations and interdetector delay volumes.

RESULTS AND DISCUSSION

Effect of detector alignment

It can be seen from eqns. 9 and 13 that the signals from the differential concentration detector, the viscometer and the light-scattering detector all have the same shape. When the sample is monodisperse the signals from all three detectors also have the same peak elution volume, and only differ in their relative areas which depends on the mass-average molecular mass. If there is any molecular mass polydispersity in the sample, eqns. 10 and 14 show that the light scattering and specific viscosity peaks are shifted to lower elution volumes although the overall shape is not changed. The amount of this shift in the light scattering signal, multiplied by the calibration curve slope, D_2, is the logarithm of the sample polydispersity.

$$\frac{M_w}{M_n} = e^{D_2(V_R - V_L)} \qquad (31)$$

In the case of the viscometer the volume shift is multiplied by the Mark–Houwink exponent.

$$\frac{M_w}{M_n} = e^{aD_2(V_R - V_V)} \qquad (32)$$

The difference between the viscometer volume shift and the light-scattering volume shift gives the Mark–Houwink exponent.

$$a = 1 - (V_\eta - V_l)D_2/\sigma_x^2 \qquad (33)$$

If the Mark–Houwink exponent is greater than one, as is the case for rigid molecules, the viscometer will be shifted more than the light scattering signal. If the exponent is negative, as is the case in some star-shaped molecules, the viscometer signal will be shifted to a larger elution volume than the RI. If $a = 0$, as is the case for particles, $V_V = V_R$.

In the case of a linear polymer with a Wesslau molecular mass distribution, the main information obtained by using a molecular mass-sensitive detector is the mass average property: molecular mass or intrinsic viscosity, and the polydispersity of the sample as shown by the relative position of the two detector peaks (eqns. 31 and 32). Because of this it is critical that the actual physical volume difference that exists between detectors is correctly compensated before the data are analyzed. Any error in this correction produces a corresponding error in the measured polydispersity. If both viscosity and light scattering are measured there will be an additional error in the measured Mark–Houwink coefficients. Fig. 4 illustrates the sensitivity of these measurements to the interdetector volume difference. An error, $D_2\Delta V_{error}$, of 0.01 corresponds to about 1 s at a flow-rate of 1 ml/min.

Effect of band broadening on measured molecular mass distributions

Band broadening and the corresponding loss of resolution causes a rotation of the calibration curve about the first moment of the mass distribution of the eluting peak. This is because the molecular mass of each elution slice approaches
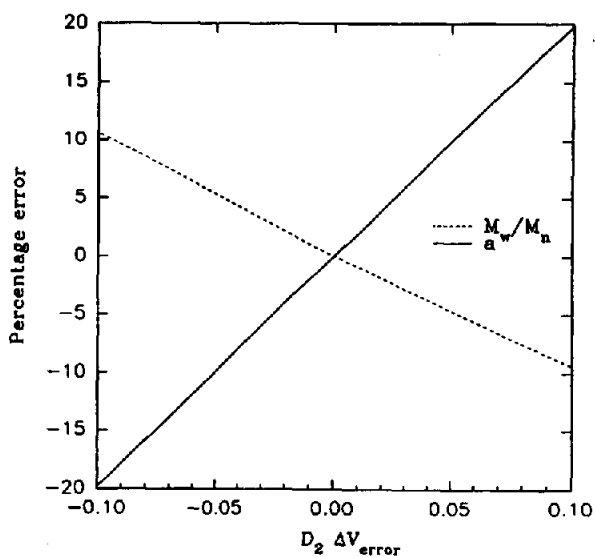

Fig. 4. Effect of errors in the determination of interdetector volume on SEC–viscometry–LS measurements of polydispersity and Mark–Houwink coefficients.

the average molecular mass of the sample. If there were no resolution, the calibration curve would be a straight line with zero slope. In practice the effect is much smaller but nevertheless it can have serious effects on the computed values. This situation is shown in Fig. 5 where the mass-average molecular mass, as measured by light-scattering, for a sample with polydispersity 2, is shown as a function of elution
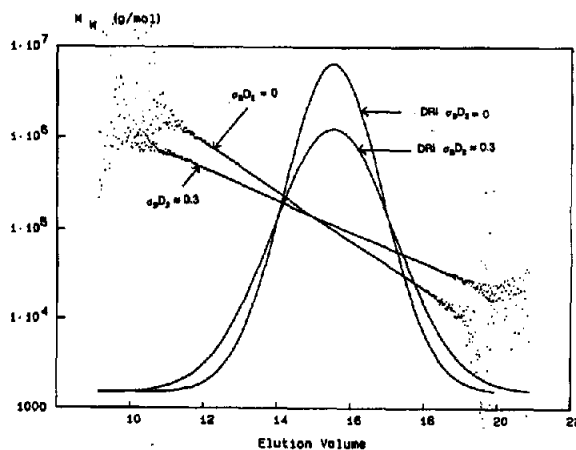

Fig. 5. Mass-average molecular mass at each elution volume, as measured by light-scattering, for a sample with polydispersity 2, for a perfectly resolved peak and for one with band broadening, $\sigma_B D_2 \approx 0.3$. Elution volume in ml. DRI = differential refractive index.

volume for a perfectly resolved peak and for one with band broadening. In the case of perfect resolution, the molecular mass measured *is* the calibration curve, with band broadening the line is less steep. Although not shown in this figure, band broadening does not alter the peak position on any of the detectors. One of the advantages of a molecular mass sensitive detector is that it

can distinguish between peak width due to polydispersity and that due to band broadening.

The effect of band broadening on the final results depends on the method of calculation used. If the molecular mass distribution is determined from the light scattering molecular mass, or from the intrinsic viscosity distribution by way of known Mark–Houwink coefficients then the effect is an apparent narrowing of the
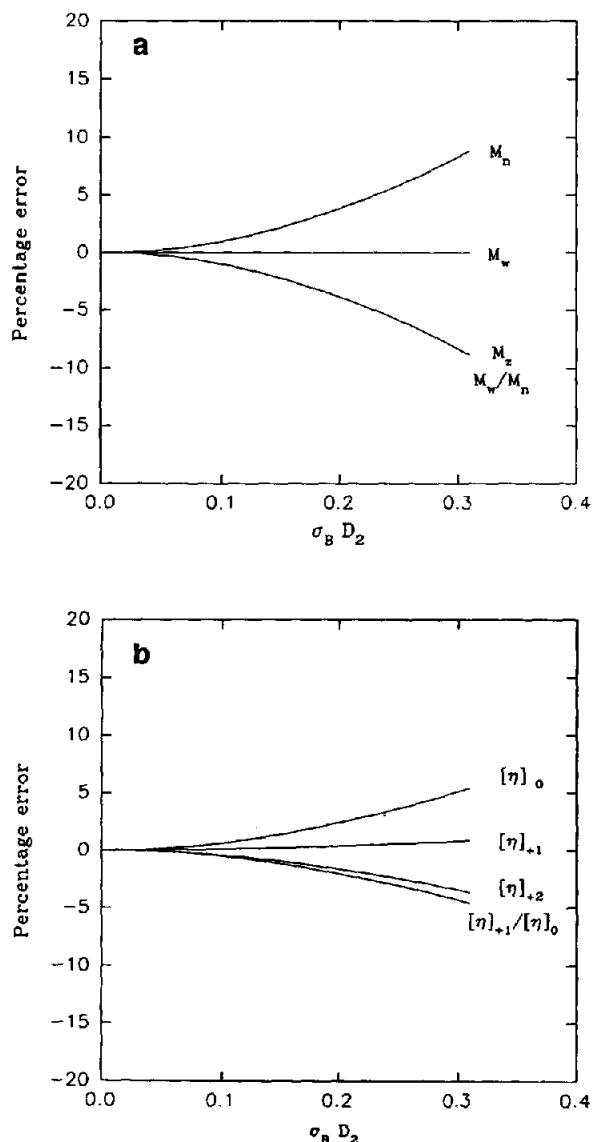

Fig. 6. Effect of band broadening for a polymer with polydispersity 2, on (a) measured moments of the molecular mass distribution by light scattering, and (b) moments of the intrinsic viscosity distribution measured by on-line viscometry.
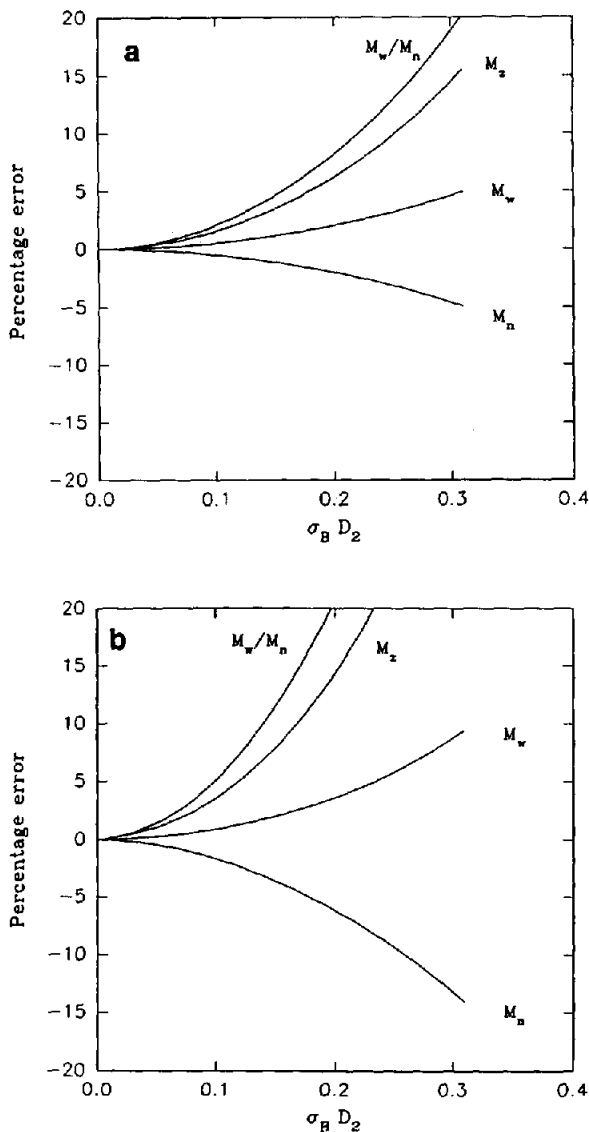
Fig. 7. Effect of band broadening for a polymer with polydispersity 2, on measured moments of the molecular mass distribution by (a) conventional SEC, and (b) universal calibration.

distribution (Fig. 6). This is because the system is losing resolution. However the mass-average molecular mass, or intrinsic viscosity are both unaffected.

By conventional SEC calibration the effect is the opposite, the peak broadening is interpreted as increased sample polydispersity (Fig. 7a). The same is true for universal calibration using on-line viscosity measurements (Fig. 7b). The relative errors caused by band broadening in this case are shown in Fig. 7. The averages determined by molecular mass sensitive detectors are less affected by band broadening than those obtained by calibration-based techniques. The measurement of molecular mass distribution by SEC–viscometry with universal calibration is the most sensitive to band broadening errors. However, if SEC–viscometry is used to measure the intrinsic viscosity distribution and then the Mark–Houwink coefficients are used to calculate the molecular mass distribution, the errors due to band broadening are the same as for SEC–LS.

Effect of band broadening on measurement of Mark–Houwink coefficients

Band broadening also has an effect on measurements of Mark–Houwink coefficients using universal calibration. When an on-line viscometer is used with universal calibration to determine the relationship between intrinsic viscosity and molecular mass, it can be shown, from eqns. 15 and 28–30 that the measured Mark–Houwink exponent, a', is given by,

$$a' = \left(\frac{1 - \sigma_B^2/\sigma_T^2}{1 + a\sigma_B^2/\sigma_T^2}\right)a \tag{34}$$

This results in an underestimate of the Mark–Houwink exponent and an overestimate of the prefactor, K.

If universal calibration is used in conjunction with light scattering, where the measured molecular mass is used with the universal calibration curve to calculate the intrinsic viscosity at each elution slice, then the situation is reversed and the Mark–Houwink exponent will be overestimated by,

$$a' = \left(\frac{a + \sigma_B^2/\sigma_T^2}{1 - \sigma_B^2/\sigma_T^2}\right) \tag{35}$$

Note that in Fig. 6 the mass-average molecular mass measured by light scattering and the mass-average intrinsic viscosity measured by on-line viscometry are unaffected by band broadening. As a result the Mark–Houwink coefficients and any determinations of molecular conformation, or branching based on them are similarly unaffected by band broadening. Fig. 8 shows the Mark–Houwink plot for a sample with polydispersity 2 with and without band broadening. In both cases, as expected, the calculated slope and intercept, a and K in eqn. 12 are the same.

Fig. 9 shows the effect of band broadening on measurements of Mark–Houwink coefficients by combined viscosity and light scattering detectors, universal calibration with a light scattering detec-
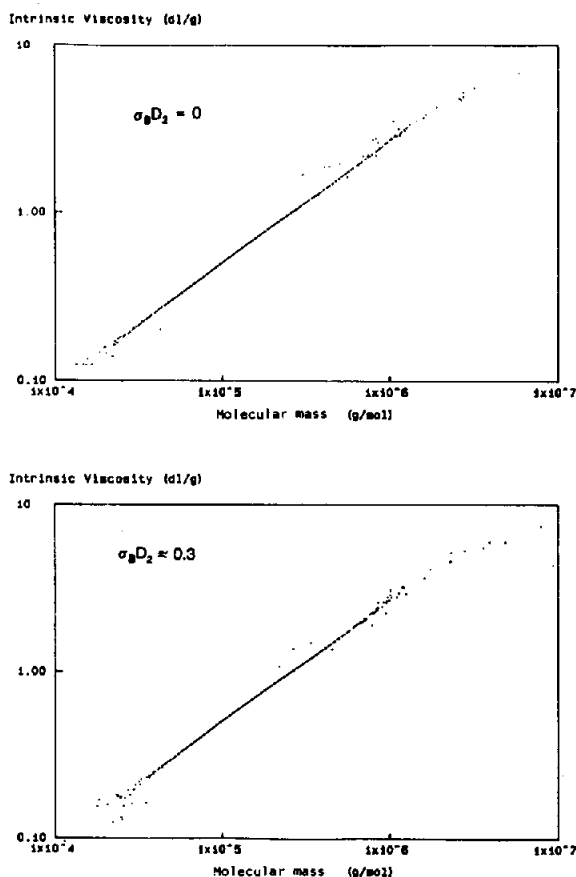

Fig. 8. Mark–Houwink plot by SEC with combined light scattering and viscometry for a sample with polydispersity 2 and $M_r \approx 150\,000$, (a) without band broadening, and (b) with band broadening, $\sigma_B D_2 \approx 0.3$. The calculated slope and intercept are the same in both cases.
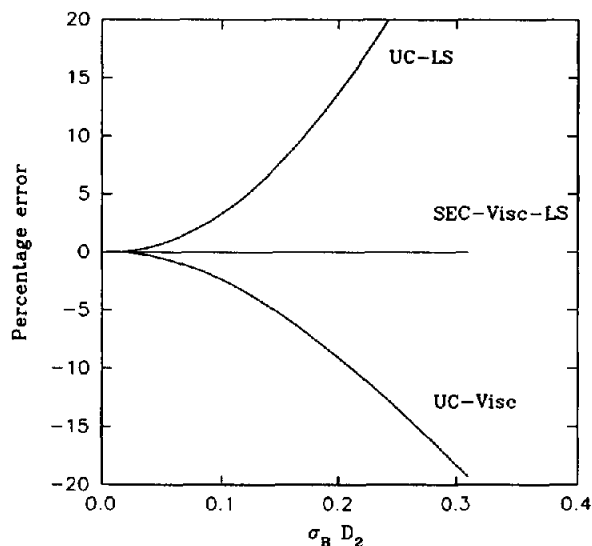
Fig. 9. Effect of band broadening on measurement of Mark–Houwink exponent, a, by different methods. UC = universal calibration.
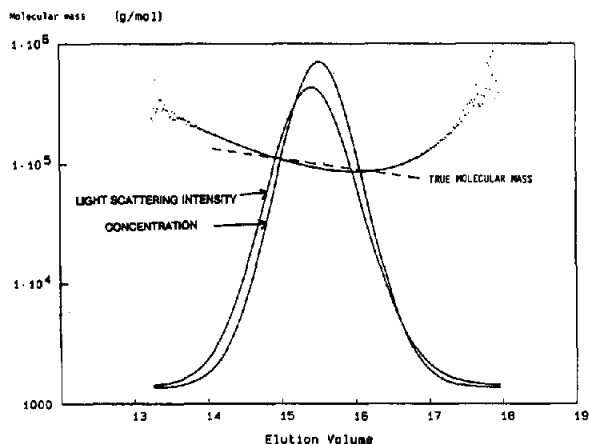

Fig. 10. Effect on the measured molecular mass at each slice of additional broadening on the light scattering detector signal, $\sigma_{add} \approx 0.06$. Elution volume in ml.
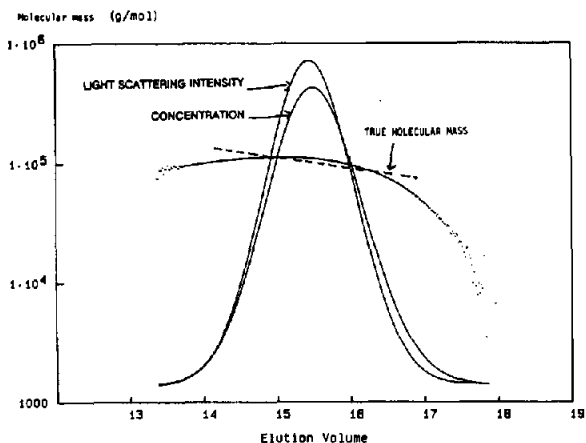

Fig. 11. Effect on the measured molecular mass at each slice of additional broadening on the concentration detector signal, $\sigma_{add} \approx 0.06$. Elution volume in ml.

tor, and universal calibration with a viscosity detector.

However, as mentioned above, the determination of the Mark–Houwink coefficients using on-line light scattering and viscosity detectors depends upon the volume delay between the three detectors being known accurately.

Effect of detector band broadening mismatch

An additional band broadening problem introduced by multiple detector systems is that the signals from different detectors are affected by differing amounts of post-column band broadening depending on the cell size and the order of detectors. When the ratio of these signals is taken to determine molecular mass and intrinsic viscosity the resultant values can be distorted. For example, if the concentration signal is the least broad, the calculated molecular masses or intrinsic viscosities for a near monodisperse sample will show a "U" shape rather than a straight line with the peak maximum molecular mass or intrinsic viscosity being underestimated (Fig. 10). Conversely if the concentration signal is the broadest the resultant values will show an "n" shape with the peak maximum molecular mass or intrinsic viscosity being overestimated (Fig. 11). This can be corrected by measuring

the differences in band broadening in each signal, and then correcting the signals using eqn. 21 to make the narrower signal equivalent to the broader one.

CONCLUSIONS

The computer model described provides a functional simulation of SEC for linear polymers. Our findings emphasize the importance of determining the correct volume offset between the concentration detector and molecular mass sensitive detectors. The results also demonstrate

that molecular mass sensitive detectors are less sensitive to band-broadening errors than are column-calibration-based methods. In particular the Mark–Houwink coefficients, and resulting branching calculations, measured by combined light scattering and viscometry, are only slightly affected by band broadening. Future work will extend the model to incorporate peak skew and polymer branching.

REFERENCES

1 W. Kaye, *Anal. Chem.*, 45 (1973) 221A.
2 A.C. Ouano and W. Kaye, *J. Polym. Sci., Polym. Chem. Ed.*, 12 (1974) 1151.
3 J.J. Kirkland, S.W. Rementer and W.W. Yau, *J. Appl. Polym. Sci.*, 48 (1991) 39.
4 W.W. Yau, *Chemtracts*, 1 (1990) 1.
5 S.T. Balke, in H.G. Barth and J.W. Mays (Editors), *Modern Methods of Polymer Characterization*, Wiley, New York, 1991, Ch. 1.
6 W.W. Yau, C. Jackson and H.G. Barth, in *Proceedings International Gel Permeation Chromatography Symposium*, San Francisco, CA, 1991.
7 C. Jackson, H.G. Barth and W.W. Yau, in *Proceedings International Gel Permeation Chromatography Symposium*, San Francisco, CA, 1991.
8 O. Prochazka and P. Kratochvil, *J. Appl. Polym. Sci.*, 31 (1986) 919.
9 O. Prochazka and P. Kratochvil, *J. Appl. Polym. Sci.*, 34 (1987) 2325.
10 F.B. Malihi, C. Kuo, M.E. Koehler, T. Provder and A.F. Kah, *ACS Symp. Ser.*, 245 (1984) 281.
11 L. Letot, J. Lesec and C. Quivoron, *J. Liq. Chromatogr.*, 3 (1980) 427.
12 J. Lesec and G. Volet, *J. Liq. Chromatogr.*, 13 (1990) 831.
13 T.H. Mourey and S.M. Miller, *J. Liq. Chromatogr.*, 13 (1990) 693.
14 R. Lew, P. Cheung, S.T. Balke and T.H. Mourey, *J. Appl. Polym. Sci.*, 47 (1993) 1685.
15 P. Cheung, R. Lew, S.T. Balke and T.H. Mourey, *J. Appl. Polym. Sci.*, 47 (1993) 1701.
16 M. Guita and O. Chiantore, *J. Liq. Chromatogr.*, 16 (1993) 633.
17 S. Pang and A. Rudin, *J. Appl. Polym. Sci.*, 46 (1992) 763.
18 F. Rodriguez, *Principles of polymer systems*, McGraw-Hill, New York, 2nd ed., 1982, Ch. 6.
19 W.W. Yau, J.J. Kirkland and D.D. Bly, *Modern Size Exclusion Liquid Chromatography*, Wiley, New York, 1979, Ch. 9.
20 P. Kratochvil, *Classical Light Scattering from Polymer Solutions*, Elsevier, New York, 1987, Ch. 3.
21 M. Bohdanecky and J. Kovar, *Viscosity of Polymer Solutions*, Elsevier, New York, 1982, Ch. 2.
22 H. Benoit, Z. Grubisic, P. Rempp, D. Decker and J.G. Zilliox, *J. Chem. Phys.*, 63 (1963) 1507.
23 W.W. Yau, H.J. Stoklosa and D.D. Bly, *J. Appl. Polym. Sci.*, 21 (1977) 1911.